On singular values decomposition and patterns for human motion analysis and simulation

Adrien Datas, Pascale Chiron and Jean-Yves Fourquet

***Abstract*— We are interested in human motion characterization and automatic motion simulation. The apparent redundancy of the humanoid w.r.t its explicit tasks lead to the problem of choosing a plausible movement in the framework of redundant kinematics. This work explores the intrinsic relationships between singular value decomposition at kinematic level and optimization principles at task level and joint level. Two task-based schemes devoted to simulation of human motion are then proposed and analyzed. These results are illustrated by motion captures, analyses and task-based simulations. Pattern of singular values serve as a basis for a discussion concerning the similarity of simulated and real motions.**

I. INTRODUCTION

Human motion generation is highly complex. Here, we are interested in a task-based approach that lead to coordination schemes for the numerous degrees of freedom (dof) of the human kinematic chain.

The work described here is devoted to the study of intrinsic properties of the mapping at kinematic level between task and joint space and to the role of optimal paths at task level. The motivation is not to neglect dynamics - essential in whole-body equilibrium for instance - but to describe a simple framework for plausible human-like motion generation, when dynamics are not decisive. The ideas are tested on sitting reach motions, for both translations and rotations task components.

Generally, a task imposes the motion of hand(s) and/or head and is denoted by the evolution in space and time of the location X of dimension m of these bodies. A reaching task consists in reaching a location X^f from X^0. The configuration q of the mechanical system is known when the value of all its n independent joints is known. If $m < n$, the motion problem is under-constrained, sometimes said "ill-posed" in human movement literature, and this setting is known as kinematic redundancy. Then, a multiplicity of joint velocities produce the same velocity in task space. The problem can be formulated as an optimization problem in configuration space and, inside this category of problems, minimum-norm solutions leads to weighted pseudo-inversion schemes.

Literature on the human movement analysis is mainly focused on reach motion and translation information. Very few works have studied the questions relative to the orientation of the hand or relative to the paths and motions in task space when translation and rotation of the end-effector are both imposed. Questions are numerous : they concern the geometry in task space (shape of paths, significant parameterization [1], [2],..), and the temporal aspects (velocity profile, sequences of reach and grasp [3], [4], [5], simultaneous evolution of translation and rotation [6], [7],...). Since coordination of translation and rotation is the focal point, time-scale and length-scale are obviously concerned. As a result of human motion studies, no "fundamental human motion principle" emerges but optimization principles have proved to be useful guides.

In this paper, the focus is on seated reaching motions. The simulations are realized with a 23 dof virtual human upper-body. In the next section, optimization principles, distances and shortest paths are studied. Section 3 presents how joint variables map into task space through their intrinsic properties and proposes two control schemes enabling to invert these maps, with or without priority, globally or independently. The motion captures are analyzed in section 4 using a robust play-back scheme. In section 5, motion simulation are compared to motion captures. Finally, a discussion and conclusion are provided.

II. OPTIMIZATION PRINCIPLES

Optimization principles have been studied in human motion literature. They can be studied in joint space, considering internal dynamics by using inertia metrics, or in task space. In this latter space, various authors have studied the reach motion in free space. The main idea is that humans favor a path in task space such that the distance to the target monotonously decreases and, even more, that the hand follows the shortest path. In fact, in many cases reported in the literature, the observed path is close to straight lines [8], [9] and the motion along the path exhibits a bell-shaped velocity profile [10], [11]. This behavior has been associated to the integral criteria in task-space that provides the *minimum hand jerk* solution [8]. But, several authors have shown that the reference path is not always a straight path and some of them attempted to define new criteria in order to explain these discrepancies [12]. On the one hand, one may think that evolution has led to render the human locomotor apparatus really efficient and turn him able to follow the most efficient paths in Cartesian world: the straight line. Remark that statistical methods popularized in industrial cycle-time measurement such as MTM implicitly include this fact since the cycle-time in usual workplaces is only related to distance of reach [13], [14], [15]. On the other hand, we know that kinematic chains are not isotropic motion

A. Datas, P. Chiron and J-Y. Fourquet are with Laboratoire Gnie de Production, LGP-ENIT, INPT, Un. de Toulouse, FRANCE {adrien.datas, pascale.chiron,jean-yves.fourquet}@enit.fr

generators in Cartesian space. Thus, intuitively, one can infer that there is a preferred workspace zone in which the path is a straight line, and other zones in which the mechanical constraints induced by the nature of kinematic chains will render really difficult to follow a straight line. Here, the matter is not so much to ask if optimization principles act in Cartesian space or in joint space [16] [17] but rather how to reproduce a trade-off between the task efficiency and the constraints induced by the mechanical structure.

A. Distance and path in $\mathbb{R}^3$ and $SO(3)$

When studying task-level description of human motion, we are mainly interested in rigid body motion where the bodies of interest are hands or head for manipulation and gaze tasks. Human manipulation tasks (touch, grasp, carry) is such that the position and orientation of the hand(s) are partially or totally known. If the task presents a symmetry, one rotation can be left free, but in many cases it is desirable to impose both translation and orientation of the hands as the result of the definition of a task.

For translation of a body-fixed point in Cartesian coordinates $X = (x, y, z)$ of a specific body (hand, head,...), the natural way to measure length and distance is to use the Euclidean metrics and the shortest path, the *geodesic*, is the straight-line. Rotations are elements of $SO(3)$ (the Special Orthogonal Group of dimension 3), a 3-dimensional differential manifold with a Lie group structure. Since Euler [18], we know that it is possible to transform a rotation matrix (or an orthonormal vector frame) R_0 into a rotation (or another vector frame) R_1 by defining a vector w around which an amount of rotation $\Theta \in [0, 2\pi)$ is performed. The geodesic on $SO(3)$ between R_0 and R_1 is the path obtained by rotating around w with a Θ amount. The distance between two rotations is the length of the geodesic between them. In SO(3), this distance d_r between two rotations R_0 and R_1 is given by:

$$d_r(R_0, R_1) = ||\text{logm}(R_0^t R_1)||_{fro}$$

where $||A||_{fro} = \text{trace}(\sqrt{A^t A}) = \sqrt{(\sum_i \sigma_i^2)}$ is the Frobenius norm of the matrix A, logm stands for the matrix logarithm and the σ_i are the singular values of A.

Then, if θ varies linearly as a function of a normed parameter τ ($\theta(\tau) = \mu\tau + \nu$), the motion is a linear interpolation from R_0 to R_1 along the geodesic [19] [18]. This simple solution is the one provided by the *slerp* algorithm [20] popularized with unit quaternions.

B. Combining rotations and translations

The task simulation amounts to the definition of the interpolation laws for both the position of a particular point of the hand (the Tool Center Point (TCP)) and the orientation of a body-fixed frame. Such a composite object lives in SE(3), the Special Euclidean group of dimension 3. On one side, one may think that translation and rotation follow their own rule, independently in two parallel spaces, $\mathbb{R}^3$ for the Cartesian coordinates, SO(3) for the orientation parameters. Intrinsic metrics and closed-form geodesics are available in each space. Following this idea leads to obtain a straight line motion in Cartesian space for the TCP and a geodesic in $SO(3)$ for the frame attached to the body. We may think that this independence is dubious. In fact, beyond the fact that this problem is solvable in a well-posed setting with natural metrics, at least two other arguments speak for this solution. Firstly, this decoupling is observed naturally in the motion of bodies taken at the center of mass: in absence of external forces, the linear and angular velocities keep constant values and the resulting path follows in parallel the geodesics of $\mathbb{R}^3$ and SO(3). Secondly, SE(3) is not the cross-product of $\mathbb{R}^3$ and SO(3) and there is no natural (i.e. no bi-invariant) metric on it [21]. Thus, choosing a metric in SE(3) requires to weight two mathematical objects of different nature with an unique measure of length. Such a weighting has no intrinsic meaning from the geometric point of view. It amounts to choose a Riemmannian metric [22] on SE(3) defining the components $(\beta_{ij}, \delta_{ij})$ and thus the length l by:

$$l = \sqrt{(\sum_{ij} \beta_{ij} v_i v_j + \delta_{ij} \omega_i \omega_j)}$$

where v_k and ω_k are respectively the linear and angular velocity components. This choice may be motivated by different reasons and the synchronization of translations and rotations may be viewed as time or/and length scale.

III. Task-based simulation schemes

A. Space mappings and associated criteria

In task space, human motion can be seen as a set of rigid body motions $X_i(t)$ for the hands and the head. Each task can be written as a function of joint coordinates $X_i = f_i(q)$ then the relation between the respective first order variations δX_i and δq, or the exact relation between the velocities $\dot{X}_i$ and $\dot{q}$, writes as a linear map:

$$\delta X_i = J_i \delta q \qquad \text{or} \qquad \dot{X}_i = J_i \dot{q} \tag{1}$$

where $J_i = J_i(q)$ is the $m_i \times n$ task Jacobian matrix associated to the task X_i. This mapping is configuration-dependent and does not provide an isotropic transformation from joint space to task space. The properties of this mapping are enlightened by its singular value decomposition (SVD) [23]. SVD provides the means to analyze the amount of joint displacement necessary to move in a given direction in task space. SVD of J_i writes:

$$J_i = U \Sigma_i V^T \tag{2}$$

where: $U = [u_1 \quad u_2 \ldots u_{m_i}]$ is an orthonormal basis for the tangent vectors to the task space, $V = [v_1 \quad v_2 \ldots v_n]$ is an orthonormal basis of the tangent space to the configuration space, $\Sigma_i = diag\{\sigma_1, \sigma_2, ..., \sigma_p\}$ is a $(m_i \times n)$ diagonal matrix with rank $p = min\{m_i, n\}$ and the singular values σ_k of J_i are arranged such that $\sigma_1 \geq \sigma_2 \geq ... \geq \sigma_p \geq 0$.

The geometrical meaning of this decomposition is: J_i maps a unit ball in the tangent space to the task space

into a p-dimensional ellipsoid in the tangent space to the configuration space. This ellipsoid has principal axes u_k with length σ_k. Remark that the $\{u_k\,; k = 1, \ldots, p \leq m_i\}$ form a basis for the range of J_i and the $\{v_k\,; k = p+1, \ldots, n\}$form a basis of the kernel of J_i.

Thus, a significant difference of value among the σ_k implies that the amount of joint displacement consumed for a given norm of displacement in task space varies with the direction and that some directions in task space are really easier to follow. A global measure of the anisotropy of the mapping is given by the manipulability index: $\mathcal{M}(q) = \sqrt{det(J_i(q)J_i^T(q))} = \sqrt{det(\Sigma_i\Sigma_i^t)} = \sigma_1\sigma_2\ldots\sigma_p$.

Thus, on the one hand, one may think that hands and gaze motion will occur along geodesics if these task paths do not require an excessive amount of joint motion. On the other hand, some configurations are such that task displacement in a certain direction requires a really high amount of joint motion: in this latter case, at least one singular value takes a significant smaller value and straight paths are not necessarily efficient.

B. Combination and prioritization of tasks

When facing various tasks, there is two main approaches:

- consider that these tasks form a global mapping and try to obtain a global least-error solution when some tasks are antagonistic or,
- consider that some tasks have higher priority, try to realize them first then obtain a least-error solution for lower priority tasks.

In this work, we study and compare both approaches with articular emphasis on the ability to tune motion around geodesics using singular value decomposition as a measure of cost of joint displacements. Initial guesses are geodesics in task space. This guess is adapted when SVD shows that the geodesic is too costly at joint level. Thus, the simulated paths are built upon optimization in task space under the condition of a reasonable expense in joint space.

C. A global task approach

In that setting, the task is built as a m-dimensional vector X of the tasks $X_i; i = 1, \ldots, l$ with $m = \sum_{i=1}^{l} m_i$. In particular, rotation and translation components enter in the definition of X. The mapping between δX and δq writes:

$$\delta X = J\delta q \tag{3}$$

where $J = J(q)$ is the $m \times n$ Jacobian matrix associated to the global task X. The control scheme is the following:

$$\boldsymbol{\delta q = J^{\#}_{W,F}\delta X + Pz} \tag{4}$$

with the weighted and filtered pseudoinverse of J [24]:

$$J^{\#}_{W,F} = W^{-1}J^t(JW^{-1}J^t + F)^{-1} \tag{5}$$

where W is the $n \times n$ inertia-weighting matrix, F stands for the $m \times m$ filtering matrix [25] computed by:

$$F = \sum_{i=1}^{m}(\alpha_i^2 u_i u_i^t)$$

where α_i switches from zero to a non-null value when σ_i is under a given threshold [26], [12], and P is the Jacobian null-space projector allowing to include equality or inequality constraints in the z term (such as joint limits assessment or convergence to a reference posture). Thus, this scheme enables to follow geodesics when the singular values σ_i are above a given threshold, and to change the path when one singular value passes below it.

D. Stacks of tasks and prioritization

It may be useful to consider a cascade of tasks with decreasing priority [27], [28], [29], the higher priority tasks remaining unchanged by the execution of the lower priority ones. This scheme is generally used to consider antagonistic tasks. In this work, we propose to adapt the above filtering technique to this paradigm in order to filter independently the different tasks, thus giving a better tuning of the task paths. For instance, moving both hands and head can be written as a cascade of three separate subtasks, or more if rotation and translation components are considered independently. In this latter case, filtering threshold can be tuned independently. That way, this scheme allows to tune independently the distance to geodesics in rotation and translation and allows to reproduce captured motions that present these features. The algorithm writes:

$$\begin{array}{l} P_0 = \mathbb{I} \\ J_A = [\,] \\ \delta q = 0 \\ \delta q_0 = 0 \\ \text{for } i = 1 \text{ to } k \\ \quad \hat{J}_i = J_i P_{i-1} \\ \quad \delta q_i = P_{i-1}\hat{J}^{\#}_{i,W,F}(\dot{X}_i - J_i\delta q_{i-1}) \\ \quad \delta q = \delta q + \delta q_i \\ \quad J_A = [J_A; J_i] \\ \quad P_i = \mathbb{I} - J^{\#}_{i,W} J_i \\ \text{endfor} \end{array} \tag{6}$$

Remark that the filtered generalized inverse $\hat{J}^{\#}_{i,W,F}$ generated at step i in this algorithm is based on the mapping $J_i P_{i-1}$where P_{i-1} is the projector associated to the first $i-1$ tasks. Thus, singular value decomposition and filtering will depend on the priority of the task.

IV. Motion capture, play-back and analysis

A. Motion capture

Motion capture is based on a sequence of Morasso [10] of reaching movements on the horizontal plane. This experiment exhibits the fact that the hand follows a straight line for several cases but that a curved path appear for some other cases. The experiment of Morasso is modified in term of orientation: for each sequence point, position and orientation of the hand are imposed as depicted at figure 1; values are

Points	X	Y	θ
A	-25	30	$+90$
B	0	25	$+45$
C	30	29	-45
D	-30	0	$+90$
E	0	0	$+45$
F	30	0	-45

TABLE I

HAND POSITIONS IN CENTIMETERS AND ORIENTATIONS IN DEGREE.

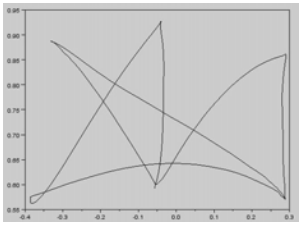

Fig. 2. Translation part of the global sequence of movements.

given in table I. Eight subjects agreed to contribute to the experiment; each one has to follow the sequence given by (7).

$$E \Rightarrow B \Rightarrow D \Rightarrow F \Rightarrow C \Rightarrow E \Rightarrow A \Rightarrow F \qquad (7)$$

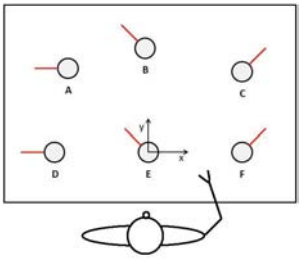

Fig. 1. Position and orientation.

In order to estimate the distance between the human trajectory and the straight line, for translation path, we use the linearity index [6] which is a usual measure in the Cartesian space. The smaller the LI is, the straighter the path is. We transpose this LI measure for the orientation and denote it DI. This DI represents the maximal distance between a given orientation and a geodesic path between two different orientations.

$$LI = D_{max}/LT \;\; ; \;\; DI = dr_{max}/DT \qquad (8)$$

where D_{max} is the maximum Euclidean distance between a point on the path and the straight line, LT is the straight line length, dr_{max} is the maximum deviation in the orientation space and DT is the distance between the orientation of the two utmost points.

The hand translation path is depicted in figure 2. For illustrating purposes, we focus here on two movements: the first one, from (E) to (A), for which the translation observed is close to a straight line, and the second one, from (D) to (F), for which this translation occurs along a curve different from a straight line. In both movements, we focus on the evolution of the hand in $\mathbb{R}^3$ and $SO(3)$. Measurements for the 8 subjects did not present significant differences considering the purpose of this paper, and the numerical values for LI and DI are the average value.

We can measure the deviation from the trajectory thanks to the LI and DI measures. We observe, for the (E) to (A) movement LI = 4.16% and DI = 40.6%. Thus human motion is close to the shortest path in translation and quite far from the geodesic in $SO(3)$. For the (D) to (F) movement, deviation measured are LI = 10.16% and DI = 10.6%. In this case, the subject did not follow the shortest path neither in Euclidean space nor in $SO(3)$. This example, among others [30], illustrates that the spatial path of the hand in translation and in orientation exhibits different features, sometimes being the shortest in translation, sometimes following the geodesic in $SO(3)$ and sometimes being far from the geodesics in both subspaces.

B. Motion playback

In order to compare simulated movement with captured one not only in task space, but also in joint space, we develop a method for motion adaptation and playback allowing the virtual human to mimic the captured movement. There are numerous algorithms for avatar animation from captured data. The main difficulty comes from the fact that human and its model (manekin) do not share the same geometric and kinematics properties. Thus, it is necessary to make technical choices to compensate for the model simplification. A classic approach is the use of a kinematic model [31], [32]; more advanced techniques take into account some dynamical constraints as in [33]. We proposed here to use the iterative procedure of the stack of tasks method in order to converge body after body to the least-error posture using only orientation data of the bodies as suggested by [26]. This method has shown to be robust to the lack of precision on body dimensions and has permitted to built joint values and associated mappings.

V. SIMULATION

The methods defined in section 3 are applied in order to simulate the sequence of the experiment described above. Results obtained for both methods are compared for the (E) to (A) and the (D) to (F) movements. In both methods, the filtering scheme is used. However, in the case of the global scheme there is a common threshold for all singular values and filtering is active when any singular value passes under this threshold. In the case of the stack of tasks scheme, threshold for translation tasks and threshold for orientation tasks can be choosen independently.

3 tasks are considered (gaze, TCP translation and hand orientation) leading to four cases in the prioritization scheme depending on the way tasks are ordered. For each case, values of LI and DI are given in table II for the (E) to (A) movement and in table III for the (D) to (F) movement.

Case	Task 1	Task 2	Task 3	LI	DI
1	Translation	Gaze	Orientation	1.62%	1.36%
2	Gaze	Translation	Orientation	1.6%	1.36%
3	Gaze	Orientation	Translation	3.35%	1.3%
4	Orientation	Gaze	Translation	3.35%	1.3%

TABLE II

STACK OF TASKS FOR THE (E) TO (A) MOVEMENT.

Case	Task 1	Task 2	Task 3	LI	DI
1	Translation	Gaze	Orientation	6.2%	0.44%
2	Gaze	Translation	Orientation	6.13%	0.44%
3	Gaze	Orientation	Translation	6.8%	0.56%
4	Orientation	Gaze	Translation	6.8%	0.56%

TABLE III

STACK OF TASKS FOR THE (D) TO (F) MOVEMENT.

A. *Trajectories results*

Simulated hand TCP path obtained for the complete sequence are given for each method and in each case in table IV. For hand paths, case 4 is the same as case 3. Thus only results for case 3 are given.

Theses results can be compared to the captured data given in figure 2. Trajectories are visually similar. We present in table V the visualisation of the (D) to (F) movement and the (E) to (A) movement for playback method and simulation with stack of tasks.

By tuning the thresholds, these figures show that it is easy to obtain similar path in translation. But some difficulties remain for the generation of changes in the orientation path with the chosen thresholds.

In order to study why the action of SVD filtering in both schemes gives interesting results in the translation case and does not allow to provide enough deviation from geodesic path in the orientation case, computation of singular values was done in captured and simulated cases.

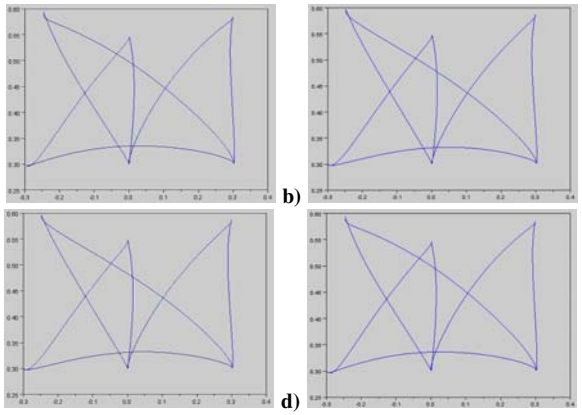

Table IV : Simulated hand translation path for different control schemes :
a) Simulated hand trajectories with global scheme.
b) Simulated hand trajectories with stack of tasks case 1 scheme.
c) Simulated hand trajectories with stack of tasks case 2 scheme.
d) Simulated hand trajectories with stack of tasks case 3 scheme.

TABLE IV

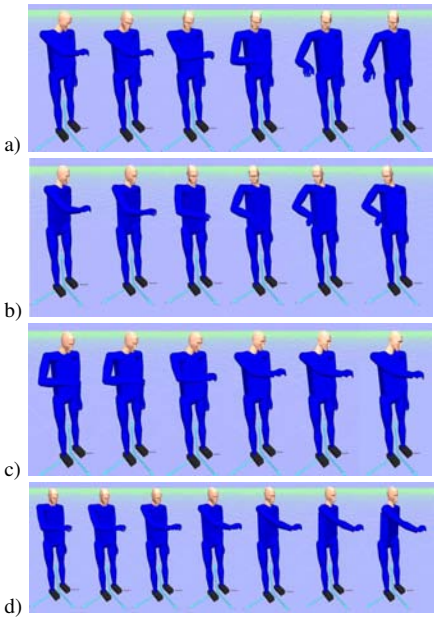

Table V : Visualisation of the movement :
a) (D) to (F) movement with play-back motion.
b) (D) to (F) movement with stack of tasks method.
c) (E) to (A) movement with play-back motion.
d) (E) to (A) movement with stack of tasks method.

TABLE V

B. *Patterns of singular values*

In a first step, singular values of the Jacobian matrix are computed with the global scheme, thus Jacobian matrix includes hand translation, hand orientation and gaze set points in task space. In the case of captured movements, the playback method is used to compute joint values, thereafter the singular values of the Jacobian matrix can be computed using the global scheme. Singular values belong to a 9-dimensional space. Results obtained for the captured and simulated movement are given in figure VI. The beginning time of each movement of the sequence are given in table VII. Pattern must be compared for each movement and thus for ad hoc extracted period. Even if it is difficult to understand if singular values correspond to the translation, the orientation or the gaze tasks, patterns are very similar and 3 groups of 3 values are observed: one around 2.1 (2.4, 2.1 and 1.9), one around 1.3 (1.4, 1.3, 1.1) and one around 0.4 (0.5, 0.4 and 0.3) for both captured and simulated movements.

In order to be able to observe the singular values for the translation task and for the orientation task, singular values are computed using the stack of tasks scheme. Thus singular values are obtained not for the global Jacobian matrix but for the Jacobian matrix associated to the task i : J_iP_{i-1}. Thus task ordering is important, for example in the case of translation task, in case 1 $J_iP_{i-1} = J_1$; in case 2 $J_iP_{i-1} = J_2P_1$: the translation is projected in the gaze task; in case 3 $J_iP_{i-1} = J_3P_2$: the translation is projected in the gaze and in the orientation tasks; and so on...

For translation, cases 1 and 2 lead to very similar results,

Situation	E ⇒ B	B ⇒ D	D ⇒ F	F ⇒ C	C⇒ E	E ⇒ A	A ⇒ F	end
Captured	1	79	141	201	254	306	364	440
Simulated	20	45	84	144	173	215	255	318

TABLE VII

BEGINNING TIME FOR EACH MOVEMENT OF THE SEQUENCE, IN CASE OF CAPTURED OR SIMULATED SITUATIONS

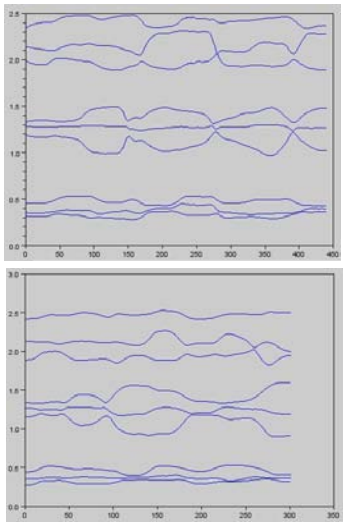

Table VI : Singular value evolution for play-back motion and standard scheme simulation :
a) Global scheme computation of the captured movement.
b) Global scheme computation of the simulated movement.

TABLE VI

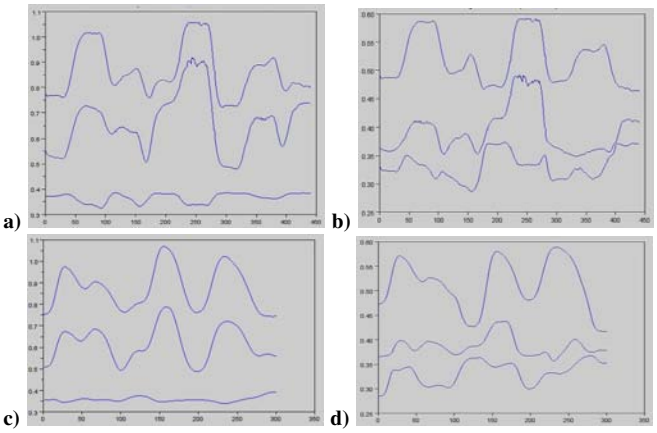

Table VIII : Singular value evolution of the translation task for both captured andsimulated movement using stack of tasks :
a) Captured movement in case 2.
b) Captured movement in case 3.
c) Simulated movement in case 2.
d) Simulated movement in case 3.

TABLE VIII

and for orientation, cases 3 and 4 lead to very similar results; thus gaze priority position is not considered as a decisive factor. This is why results are given for cases 2 and 3 only, allowing to compare translation and orientation priority position. First of all, singular values of Jacobian matrix associated to the translation task are given in figures of table VIII for captured and simulated movement cases 2 and 3 respectively. Captured and simulated patterns of singular values exhibits the same profiles. The 3 different singular values mean and extremum values are of same order in case 3 and case 2, however values decrease between cases 2 and 3. The similarity of patterns shows the effectiveness of the simulation scheme and the differences in value depending on the order of priority illustrates the fact that ability to provide a displacement in task space depends on the order of priority of the task.

Singular values of Jacobian matrix associated to the rotation task are given in figures of table IX for captured and simulated movement cases 3 and 2.

Captured and simulated patterns of singular values exhibit a similar profile, even if profiles are smoother for simulated cases. Profiles obtained in case 3 or in case 2 are difficult to compare. The singular values are higher than in the translation case, their magnitude are very different (in case 2: from 0.32 to 1.1 for translation and from 0.75 to 2.0 for rotation; in case 3: from 0.27 to 0.6 for translation and from 1.3 to 2.3 for rotation). Thus, the stack of tasks scheme seems to be more adapted because it allows for taking into account different thresholds.

C. Summary of simulation results

Simulation schemes proposed herein, based either on global inverse kinematics or stack of tasks methods, allow for reproducing the Cartesian paths of the hand (obviously for translation tasks). Consequently, the filtering based on the singular values of the Jacobian matrix is adapted and allows to understand in a purely kinematic way the trajectory deviation from the straight line. However, the filtering scheme must be adapted for the orientation tasks. Indeed, captured movements show large deviation from the geodesic path, which are not reproduced in our simulated movements.

VI. DISCUSSION

Herein were proposed two simulation schemes allowing to reproduce human movements including a SVD filtering scheme providing potential trajectories deviation from geodesics. Moreover, a motion adaptation and play-back method was proposed in order to compute joint values for captured movements and permitted to compare their values with simulation results ones.

The pattern of singular values for both tasks where studied. The simulation schemes are adapted for reproducing translation tasks even when the trajectory deviates from the straight line. However the scheme and its actual settings do

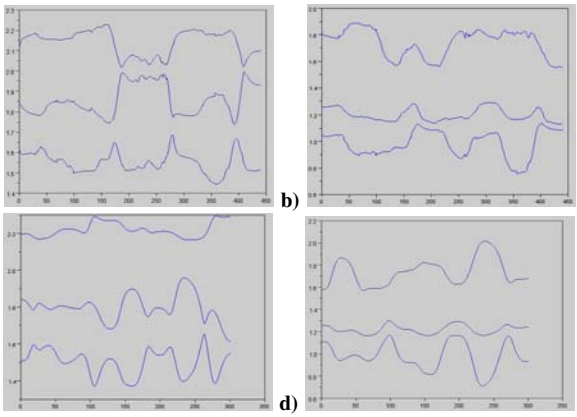

Table IX : Singular value evolution of the rotation task for captured and simulated movement using stack of tasks :
a) Captured movement in case 3.
b) Captured movement in case 2.
c) Simulated movement in case 3.
d) Simulated movement in case 2.

TABLE IX

not allow to produce enough deviation from the geodesic path in orientation.

The global scheme allows to adjust a global filter based on the singular values of the mapping from joint space to SE(3). The stack of tasks scheme including prioritization allows to adjust the threshold independently for the different tasks i.e. orientation and translation. Thus this last scheme should be preferred to simulate movement including both tasks but it needs further study.

Further improvement will particularly focus on the orientation task by defining adapted threshold values, providing new profiles for filtering and studying filtering not only based on singular value but taking into account distance to articular limits in the cost to consider.

REFERENCES

[1] S.B. Choe and J.J. Faraway. Modeling head and hand orientation during motion using quaternions. *Proceeding of the SAE Digital Human Modeling for Design and Engineering Conference*, June 15-17 2004.

[2] M.R. Pierrynowski and K.A. Ball. Oppugning the assumptions of spatial averaging of segment and joint orientations. *Journal of Biomechanics*, 42:375–378, 2009.

[3] F. Lacquaniti and J.F. Soechting. Coordination of arm and wrist motion during a reaching task. *The Journal of Neuroscience*, 2(4):399–408, 1982.

[4] J. Fan, J. He, and S.I. Helms Tillery. Control orientation and arm movement during reach and grasp. *Experimental Brain Research*, 171(3):283–296, 2006.

[5] C. Hesse and H. Deubel. Changes in grasping kinematics due to different start postures of the hand. *Human Movement Science*, 28(4):415 – 436, 2009.

[6] X. Wang. Three-dimensional kinematic analysis of influence of hand orientation and joint limits on the control of arm postures and movements. *Biological Cybernetics*, 80:449–463, 1999.

[7] N. Bennis and A.R. Brami. Coupling between reaching movement direction and hand orientation for grasping. *Brain Research*, 952(2):257 – 267, 2002.

[8] T. Flash and N. Hogan. The coordination of arm movements: An experimentally confirmed mathematical model. *Journal of Neuroscience*, 5(7):1688–1703, 1985.

[9] J.F. Soechting and F. Lacquaniti. Invariant characteristics of a pointing movement in man. *The Journal of Neuroscience*, 1(7):710–720, 1981.

[10] P. Morasso. Spatial control of arm movements. *Experimental Brain Research*, 42:223–227, 1981.

[11] C.G. Atkeson and J.M. Hollerbach. Kinematic features of unrestrained arm movements. *Journal of Neuroscience*, 5:2318–2330, 1985.

[12] V. Hue, J.Y. Fourquet, and P. Chiron. On realistic human motion simulation for virtual manipulation tasks. In *10th International Conference on Control, Automation, Robotics and Vision*, pages 167 –172, dec. 2008.

[13] G. J. Stegemerten H. B. Maynard and J. L. Schwab. *Methods-time measurement*. McGraw-Hill industrial organization and management series, N. Y., 1948.

[14] J. Laring, M. Forsman, R. Kadefors, and R. Ortengren. Mtm-based ergonomic workload analysis. *International Journal of Industrial Ergonomics*, 30(3):135 – 148, 2002.

[15] L. Ma, W. Zhang, H. Fu, Y. Guo, D. Chablat, and F. Bennis. A framework for interactive work design based on digital work analysis and simulation. *Human Factors and Ergonomics in Manufacturing and Service Industries*, abs/1006.5226, 2010.

[16] S.A. Engelbrecht. Minimum principles in motor control. *Journal of Mathematical Psychology*, 45:497–542, 2001.

[17] M. Svinin, Y. Masui, Z-W. Luo, and S. Hosoe. On the dynamic version of the minimum hand jerk criterion. *J. Robot. Syst.*, 22:661–676, 2005.

[18] R.M. Murray, S. Sastry, and L. Zexiang. *A Mathematical Introduction to Robotic Manipulation*. CRC Press, Inc., Boca Raton, FL, USA, 1994.

[19] F.C. Park and B. Ravani. Smooth invariant interpolation of rotations. *ACM Trans. Graph.*, 16(3):277–295, 1997.

[20] K. Shoemake. Animating rotation with quaternion curves. *SIGGRAPH Comput. Graph.*, 19(3):245–254, 1985.

[21] M. Zefran and V. Kumar. Planning of smooth motions on se(3). In *Proceedings of the 1996 IEEE International Conference on Robotics and Automation*, Minneapolis, Minnesota, April 1996.

[22] S. Arimoto, M. Yoshida, M.Sekimoto, and K. Tahara. A Riemannian geometry approach for control of robotic systems under constraints. *SICE Journal of Control, Measurement, and System Integration*, 2(2):107–116, 2009.

[23] G.H. Golub and C.F. Van Loan. *Matrix computations*. John Hopkins studies in Mathematical Sciences, 1983.

[24] Ben-Israel A. and Greville T. *Generalised inverses : theory and applications*. 2003.

[25] A.A. Maciejewski. Motion simulation: Dealing with the ill-conditioned equations of motion for articulated figures. *IEEE Comput. Graph. Appl.*, 10(3):63–71, 1990.

[26] Paolo Baerlocher. *Inverse kinematics techniques of the interactive posture control of articulated figures*. PhD thesis, Lausanne, 2001.

[27] Nakamura Y. *Advanced robotics, redondancy and optimization*. 1991.

[28] B. Siciliano and J.-J.E. Slotine. A general framework for managing multiple tasks in highly redundant robotic systems. In *Advanced Robotics, 1991. 'Robots in Unstructured Environments', 91 ICAR., Fifth International Conference on*, pages 1211 –1216 vol.2, june 1991.

[29] Oussama Kanoun, Florent Lamiraux, Pierre-Brice Wieber, Fumio Kanehiro, Eiichi Yoshida, and Jean-Paul Laumond. Prioritizing linear equality and inequality systems: Application to local motion planning for redundant robots. In *Robotics and Automation, 2009. ICRA '09. IEEE International Conference on*, pages 2939 –2944, may 2009.

[30] A. Datas, P. Chiron, and J.Y. Fourquet. On least-cost path for realistic simulation of human motion. In *1st International Conference on Digital Human Modeling, DHM 2011, Lyon, France*, june. 2011.

[31] Michael Gleicher. Retargetting motion to new characters. In *Proceedings of the 25th annual conference on Computer graphics and interactive techniques*, SIGGRAPH '98, pages 33–42, New York, NY, USA, 1998. ACM.

[32] Keith Grochow, Steven L. Martin, Aaron Hertzmann, and Zoran Popović. Style-based inverse kinematics. In *ACM SIGGRAPH 2004 Papers*, SIGGRAPH '04, pages 522–531, New York, NY, USA, 2004. ACM.

[33] Richard Kulpa. *Adaptation interactive et performante des mouvements dhumanoïdes synthétiques : aspects cinématique, cinétique et dynami*. PhD thesis, 2005.